Progress In Electromagnetics Research B, Vol. 20, 225–244, 2010

TRIPLE-BAND PRINTED DIPOLE ANTENNA WITH SINGLE-BAND AMC-HIS

M. Abu, M. K. A. Rahim, O. Ayop, and F. Zubir

Radio Communication Engineering Department (RaCED)
Universiti Teknologi Malaysia (UTM)
81310 Skudai, Johor Bahru, Malaysia

Abstract—In this paper, the designed of triple-band printed dipole antennas are incorporated with single-band artificial magnetic conductor (AMC). The single-band AMCs are designed to resonate at 0.92 GHz, 2.45 GHz and 5.8 GHz using TLC-32 dielectric substrate. The four important parameters in AMC high impedance surface (HIS) design are also described in this paper. By simulating a unit cell of the AMC structure using a transient solver in Computer Simulation Technology (CST) software, the characteristic of the AMC can be characterized. The AMC condition is characterized by the frequency or frequencies where the magnitude of the reflection coefficient is +1 and its phase is 0°. It has high surface impedance (Z_s) and it reflects the external electromagnetic waves without the phase reversal. This characteristic of AMC enables the printed dipole to work properly when the antenna with AMC ground plane (GP) is directly attached to the metal object. The performances of the antenna with and without AMC structure as a ground plane to the antenna such as return loss, realized gain, radiation efficiency, radiation pattern and directivity are studied. Reported results show that the performances of the antenna are improved. Hence, the designed dipole tag antenna can be used for metal object identifications when the AMC structure is introduced as a ground to the antenna. The properties of the antenna are also remained well when the size of metal plate attached to them is increased.

1. INTRODUCTION

In recent years, there has been increasing interest in investigating metamaterial structures that exhibit novel electromagnetic properties not found in nature. The metamaterial structures include the artificial

Corresponding author: M. Abu (maisarah@utem.edu.my).

magnetic conductor (AMC) which is known as perfect magnetic conductor (PMC). It has high impedance surface exhibits a reflectivity of +1 oppose to a perfect electric conductor (PEC) which has a reflectivity of −1 [1–4]. The AMC condition is characterized by the frequency or frequencies where the phase of the reflection coefficient is zero degrees. The AMC structure has reflected wave in phase with the incident wave. Multi-band and W-band AMC structures were proposed in [5, 6] and the details about simulation of high impedance surface using time-domain solver can be found in [7]. These high impedance structures have also been shown to reduce the surface waves, to smooth the radiation patterns and to reduce the mutual coupling in array antenna [8].

The comparative study on various artificial magnetic conductors for low-profile antenna was done in [9]. They found that the mushroom-like electromagnetic band gap (EBG) has wider bandwidth than uni-planar compact EBG, Peano curve of order 1 and Hilbert curve of order 2. While in [10], it introduces a probe fed patch antenna surrounded by high impedance surface structure to get more antennas' directivity. In [11, 12], the slots on mushroom EBG structures [1, 2] are applied to get the multiple band-gap. The characteristic of high impedance structure, which is band gap, was analyzed in [13]. A transmission line method was used to study the band-gap of the HIS structure. With absent of vias, there are no band-gap appear at the specific frequency range. But, with the design of uni-planar compact EBG proposed in [8, 9, 14], the band-gap was appeared but the vias were replaced by a thin of conductor line.

In Radio Frequency Identification (RFID) system, the tag antenna gain is the important parameter for the reading distance. The range is largest in the direction of maximum gain, which is fundamentally limited by the size and radiation pattern of the antenna [15, 16]. Various structures of dipole antenna are proposed for RFID and wireless Local Area Network (WLAN) applications [17–20]. Generally, the label-fabricated dipole tag antenna can not work on metallic surface. To overcome this problem, two types of tag design for metallic objects were proposed in [21]. They proposed printed inverted-F antenna (PIFA) and patch antenna with electromagnetic band-gap. The effects of metallic plate size on UHF passive tag performance also were studied in [22]. From the research done, they conclude that the performance of the tag antennas were still too dependent on the dimensions of the metallic plates close to them. As stated in [23], the tag performance mainly due to various kinds of platform materials can be prevented and the antenna gain also can be increased when AMC is used a ground plane to the low-profile antenna. The

AMC structure was studied in [24] to make a low-profile passive radio frequency identification (RFID) tag whose performance is tolerant to various platform materials such us lossy liquids and metallic objects.

In this paper, the triple-band printed dipole antennas proposed in [25] are applied. These antennas are constructed based on a printed triple-band monopole antenna that was proposed in [26]. The developed antenna is then incorporated with single-band AMC-HIS operating at 0.92 GHz, 2.45 GHz and 5.8 GHz. In order to verify the antenna with AMC-HIS ground plane (GP) can be used for metal object identifications; the antenna with single-band AMC-HIS GP then is incorporated with two different sizes of metal plates. The performances of the antenna at respective frequencies are studied including the return loss, realized gain, radiation efficiency and directivity. So, this paper aims to introduce the triple band printed dipole tag antennas with high impedance surface structure for metal object identifications.

This paper is structured as follows; Section 1 presents the literature review of the paper. Section 2 will explain briefly the triple band dipole antenna design, which is straight and meandered structures, followed by Section 3, where the design of single-band AMC-HIS is described. Section 4 and Section 5 introduce triple-band dipole antennas with single-band AMC-HIS. In this chapter, the properties of the antenna with and without AMC-HIS GP are discussed in detail. The properties of the antenna with AMC-HIS GP attached to two different sizes of metal plates are also described in this section. Finally some conclusions are drawn in Section 6.

2. TRIPLE-BAND PRINTED DIPOLE ANTENNA DESIGN

In this paper, the proposed antennas in [25] are applied in investigating the performances of the printed dipole antennas with and without single-band AMC-HIS structure as their ground plane. Then, it is followed by investigating the performances of the antenna with AMC-HIS GP attached directly to the metal plate.

The triple-band dipole was printed on one side of the RF-35 substrate which has a dielectric constant, $\varepsilon_r = 3.5$, thickness, $d = 0.508$ mm and tangent loss, $\delta = 0.0019$. In order to achieve a triple-band operation, the prime dipole antenna (operating at 0.92 GHz) was connected to the two branch elements, which act as an additional resonator to resonate at 2.45 GHz and 5.8 GHz. In the second design, the length of the prime dipole was meandered to reduce the antenna size. A 2.0 mm gap at the centre of the antenna is connected by a

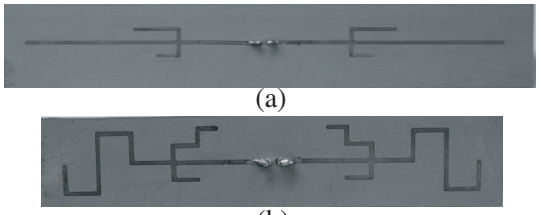

Figure 1. The structure of the proposed triple-band printed dipole antennas: (a) triple-band straight printed dipole antenna and (b) triple-band meandered printed dipole antenna [25].

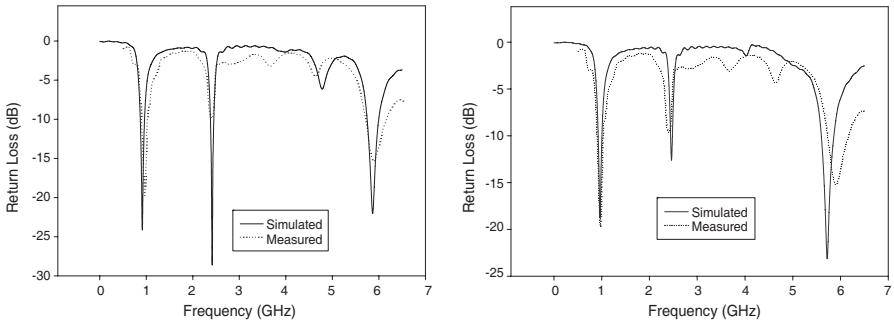

Figure 2. The simulated and measured return loss of triple-band printed dipole antennas: (a) triple-band straight printed dipole antenna and (b) triple-band meandered printed dipole antenna.

discrete port of 50 Ω. The structures of the designed antennas are shown in Figure 1.

Figure 2 shows the simulated and measured return loss of the dipole antennas. The designed antennas are operating at three different frequencies; at 0.92 GHz, 2.45 GHz and 5.8 GHz.

3. SINGLE-BAND AMC-HIS DESIGN

The presented AMC structure composed the capacitive frequency selective surface (FSS) backed by a ground plane or perfect electric conductor (PEC). The reflection phase is simulated using a time-domain solver in CST Microwave Studio. In the simulation, it requires a lattice with periodic boundary conditions and a probe to record the total electromagnetic time response. The actual (AMC) structure, PEC structure and vacuum structure are simulated step by step. Then the graph of reflection phase is obtained by applying and running a

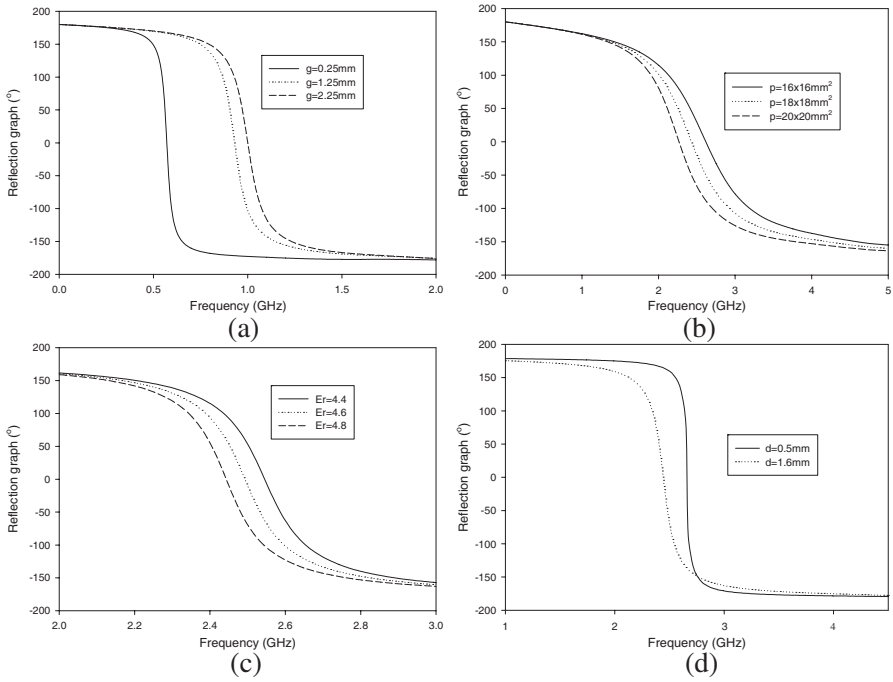

Figure 3. The reflection graph when: (a) gap size, (b) patch size, (c) substrate permittivity and (d) substrate thickness of unit cell of AMC-HIS is varied.

Table 1. Four important parameters in AMC-HIS design.

	Resonant frequency	Bandwidth
↑ Gap size (g)	↑	↑
↑ Patch size (p)	↓	↓
↑ Substrate permittivity (Er)	↓	↓
↑ Substrate thickness (d)	↓	↑

program in the VBA macro. Figure 3 illustrates the reflection phase graph (in degrees) across frequency (in GHz). The graphs show the important parameters in AMC design. They are gap between a unit cell or lattice, patch size, substrate permittivity and substrate thickness. Table 1 summarizes the effect on resonant frequency and bandwidth of the AMC when these parameters are varied. The percentage bandwidth of the AMC is determined by:

$$BW = \frac{f_u - f_L}{fc} \times 100\% \tag{1}$$

where f_u is the upper frequency such that the reflection phase equals $-90°$, f_L is the lower frequency where the reflection phase equals $+90°$ and f_C is the centre frequency where the reflection phase equals $0°$.

Figure 3(a) plots the reflection graph of the AMC when the gap size is varied from 0.25 mm to 2.25 mm with all other values remain the same. The effect of increasing the gap width is an increase in both resonant frequency and bandwidth. While, Figure 3(b) shows that as the patch size is increased both the resonant frequency and bandwidth are reduced. As can be seen in Figure 3(c), it shows that as the substrate permittivity is increased both the resonant frequency and bandwidth are also reduced. Next, Figure 3(d) shows that as the substrate thickness is increased the resonant frequency is reduced and the bandwidth is increase. So, from the given reflection graph in Figure 3 and data in Table 1, it indicates that the substrate selectivity is important in order to achieve the design goal. At low frequencies, the thicker substrate is needed because the bandwidth is become narrower. The dimension of the AMC is larger if compared to the mushroom EBG that has a via at the center of the square patch. This is because; with via the unit cell size of the EBG at the specific frequency can be reduced and the band gap can be appeared.

A unit cell of the designed single-band AMC-HIS and its reflection graph are shown in Figure 4. The AMCs are designed to resonate at 0.92 GHz, 2.45 GHz and 5.8 GHz. The square patch AMC structures are designed using TLC-32 dielectric substrate with permittivity of 3.2 and thickness of 6.35 mm. 0.92 GHz AMC-HIS has a patch size of $67.5 \times 67.5\,\text{mm}^2$ with gap size of 1.25 mm, 2.45 GHz AMC-HIS has a patch size of $18 \times 18\,\text{mm}^2$ with gap size of 1 mm and 5.8 GHz AMC-HIS has a patch size of $4 \times 4\,\text{mm}^2$ with gap size of 1.75 mm respectively.

4. A TRIPLE-BAND STRAIGHT PRINTED DIPOLE ANTENNA WITH SINGLE-BAND AMC-HIS

The designed single-band AMC-HIS then is incorporated with the triple-band dipole antennas. The performances of the antenna are studied such as return loss, realized gain, radiation efficiency, radiation pattern and directivity. In this paper, the performance of the antennas with 2×1 0.92 GHz AMC-HIS GP, 6×1 2.45 GHz AMC-HIS GP and 16×1 5.8 GHz AMC-HIS GP are investigated (see Figure 5). In order to prove that the designed dipole tag antenna with AMC-HIS GP can be used for metal object identification, the performances of the antenna with AMC-HIS GP attached to the metal plate are also investigated. So, this research begins with study the performance of the antenna with PEC GP. For an equivalent comparison, the PEC structure has same dimension of the AMC structure (length $\times$ width $\times$ thickness).

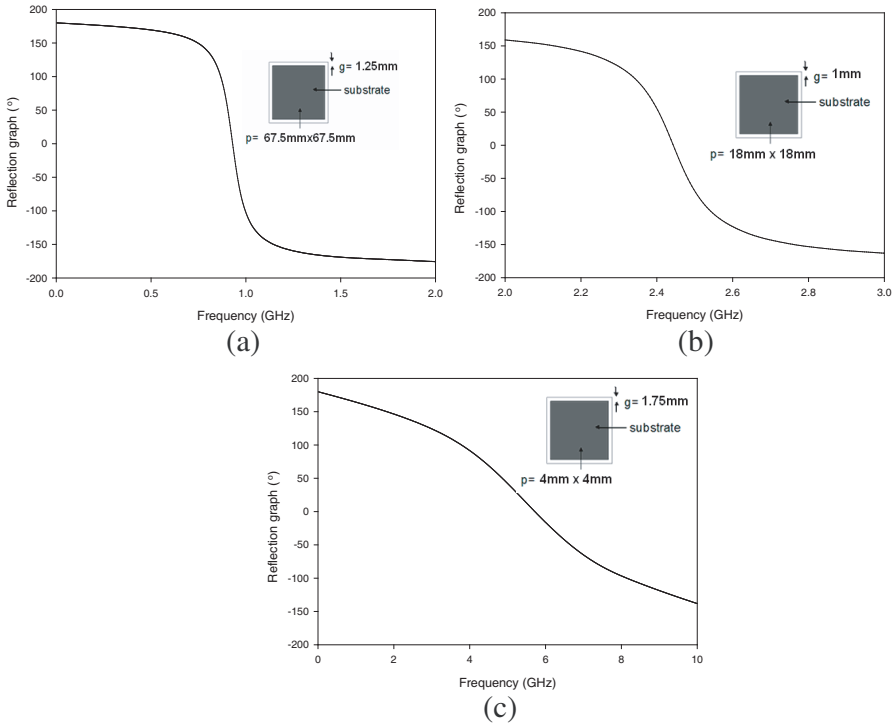

Figure 4. Reflection graph of single-band AMC: (a) 0.92 GHz AMC-HIS, (b) 2.45 GHz AMC-HIS and (c) 5.8 GHz AMC-HIS.

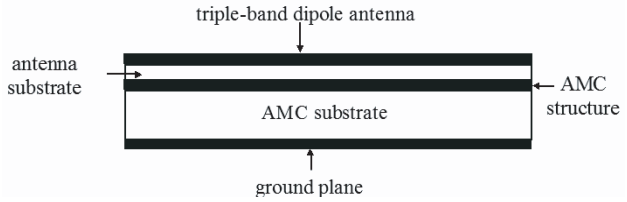

Figure 5. The structure of triple-band dipole antenna with single-band AMC-HIS GP.

The graphs of calculated input return loss, radiation pattern, realized gain and radiation efficiency for triple-band straight printed dipole antenna, antenna with single-band AMC-HIS GP, antenna with PEC GP, antenna with single-band AMC-HIS GP attached to 250 mm × 250 mm and 500 mm × 500 mm metal plates are shown in Figure 6 to Figure 8. The all obtained data are recorded in Table 2 to Table 4.

Table 2. The performance of triple-band straight dipole antenna at 0.92 GHz.

	Return loss (dB)	Realized gain (dB)	Radiation Efficiency (%)	Directivity (dBi)
Triple-band straigh dipolet antenna	−23.57	1.91	99.46	1.95
Triple-band straight dipole antenna with PEC GP	−0.06	−25.24	5.71	5.91
Triple-band straight dipole antenna with 0.92 GHz AMC-HIS GP	−10.16	5.20	96.01	5.82
Triple-band straight dipole antenna with 0.92 GHz AMC-HIS GP and 250 mm × 250 mm metal plate	−5.64	5.39	93.36	5.66
Triple-band straight dipole antenna with 0.92 GHz AMC-HIS GP and 500 mm × 500 mm metal plate	−5.65	4.89	93.04	5.21

Table 3. The performance of triple-band straight dipole antenna at 2.45 GHz.

	Return loss (dB)	Realized gain (dB)	Radiation Efficiency (%)	Directivity (dBi)
Triple-band straight dipole antenna	−10.47	2.00	91.44	2.80
Triple-band straight dipole antenna with PEC GP	−0.10	−21.10	8.90	5.66
Triple-band straight dipole antenna with 2.45 GHz AMC-HIS GP	−14.70	7.30	92.83	7.78
Triple-band straight dipole antenna with 2.45 GHz AMC-HIS GP and 250 mm × 250 mm metal plate	−7.43	9.38	90.21	9.84
Triple-band straight dipole antenna with 2.45 GHz AMC-HIS GP and 500 mm × 500 mm metal plate	−7.46	9.25	90.24	9.71

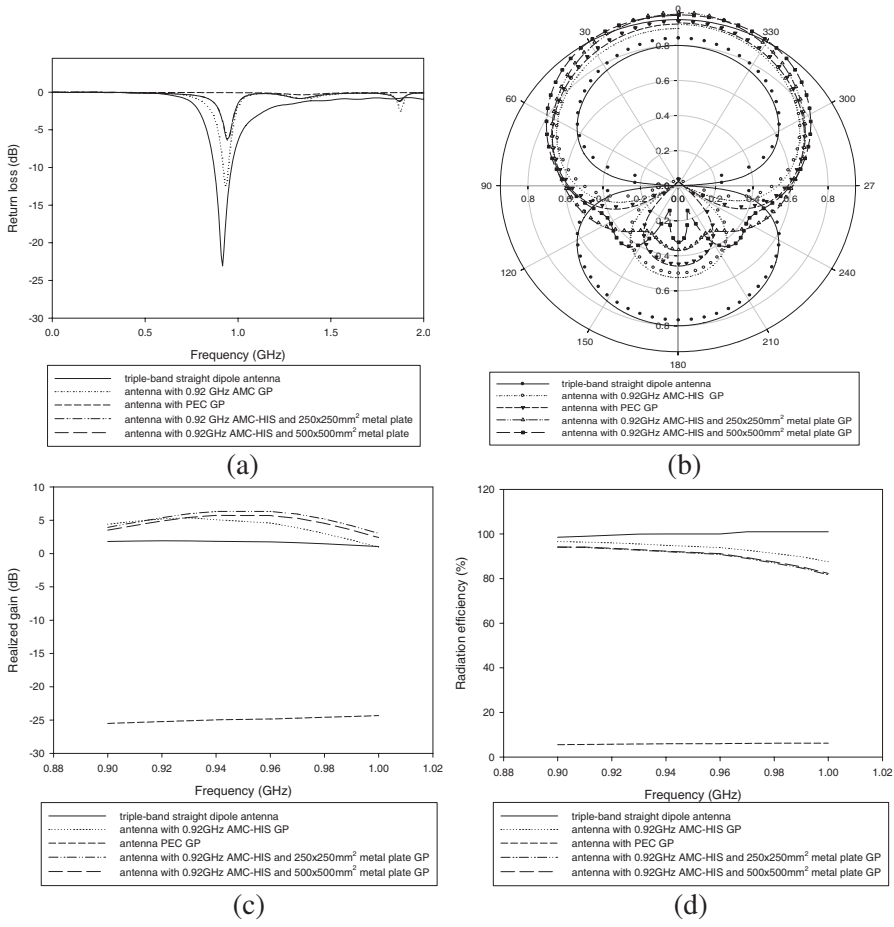

Figure 6. The performance of triple-band straight dipole antenna at 0.92 GHz: (a) return loss, (b) radiation pattern, (c) realized gain and (d) radiation efficiency.

Figure 6(a) is a plot illustrating the input return loss of the antenna studied at 0.92 GHz. At the first working frequency, the dipole antenna is resonated very well with input return loss of 23.57 dB. But, when the antenna is attached to the PEC, the input return loss of the antenna become very poor (−0.06 dB). The radiation properties of the antenna such as realized gain and radiation efficiency are also become worst. Fortunately, the directivity is increased because the metal is act as a reflector. But, when the AMC-HIS is introduced as a ground plane to the printed dipole antenna, the radiation properties are improved significantly (see Figure 6(c) and Figure 6(d)). Without the AMC-HIS, the realized gain of the antenna is 1.91 dB and with the

AMC-HIS it is increased to 5.20 dB. This is because; with AMC GP the radiation efficiency of the dipole antenna can be improved. When the antenna with AMC-HIS GP is attached to the 250 mm × 250 mm metal plate, the performances of the antenna are remained well although the metal plate size is increased to 500 mm × 500 mm. As can be seen in Figure 6(b), the radiation pattern of the antenna is changed from omni to directional; hence it increase the directivity of the antenna. The performances of the antenna studied are almost similar at 2.45 GHz and 5.8 GHz.

Table 4. The performance of triple-band straight dipole antenna at 5.8 GHz.

	Return loss (dB)	Realized gain (dB)	Radiation Efficiency (%)	Directivity (dBi)
Triple-band straight dipole antenna	−14.73	3.00	98.45	3.22
Triple-band straight dipole antenna with PEC GP	−0.94	−5.13	42.41	5.71
Triple-band straight dipole antenna with 5.8 GHz AMC-HIS GP	−17.79	7.65	96.29	7.88
Triple-band straight dipole antenna with 5.8 GHz AMC-HIS GP and 250 mm × 250 mm metal plate	−22.69	8.13	95.97	8.33
Triple-band straight dipole antenna with 5.8 GHz AMC-HIS GP and 500 mm × 500 mm metal plate	−22.82	7.91	95.94	8.12

5. A TRIPLE-BAND MEANDERED PRINTED DIPOLE ANTENNA WITH SINGLE-BAND AMC-HIS

In this section, the graphs of calculated input return loss, radiation pattern, realized gain and radiation efficiency for triple-band meandered printed dipole antenna, antenna with 2 × 1 0.92 GHz, 5 × 1 2.45 GHz, 10 × 1 5.8 GHz AMC-HIS GP, antenna with PEC GP, antenna with single-band AMC-HIS GP attached to 250 mm × 250 mm and 500 mm × 500 mm metal plates are shown in Figure 9 to Figure 11. Their performances also are summarized in Table 5 to Table 7.

Table 5. The performance of triple-band meandered dipole antenna at 0.92 GHz.

	Return loss (dB)	Realized gain (dB)	Radiation Efficiency (%)	Directivity (dBi)
Triple-band meandered dipole antenna	−8.80	1.49	97.82	1.93
Triple-band meandered dipole antenna with PEC GP	−0.06	−26.89	13.96	5.83
Triple-band meandered dipole antenna with 0.92 GHz AMC-HIS GP	−11.79	5.31	95.74	5.81
Triple-band meandered dipole antenna with 0.92 GHz AMC-HIS GP and 250 mm × 250 mm metal plate	−9.02	6.83	86.93	7.87
Triple-band meandered dipole antenna with 0.92 GHz AMC-HIS GP and 500 mm × 500 mm metal plate	−9.42	6.32	91.77	6.68

Table 6. The performance of triple-band meandered dipole antenna at 2.45 GHz.

	Return loss (dB)	Realized gain (dB)	Radiation Efficiency (%)	Directivity (dBi)
Triple-band meandered dipole antenna	−12.45	1.42	84.35	2.42
Triple-band meandered dipole antenna with PEC GP	−0.07	−23.72	−11.50	3.46
Triple-band meandered dipole antenna with 2.45 GHz AMC-HIS GP	−10.31	6.22	94.52	6.89
Triple-band meandered dipole antenna with 2.45 GHz AMC-HIS GP and 250 mm × 250 mm metal plate	−5.86	7.90	92.26	9.55
Triple-band meandered dipole antenna with 2.45 GHz AMC-HIS GP and 500 mm × 500 mm metal plate	−5.87	7.93	92.29	9.58

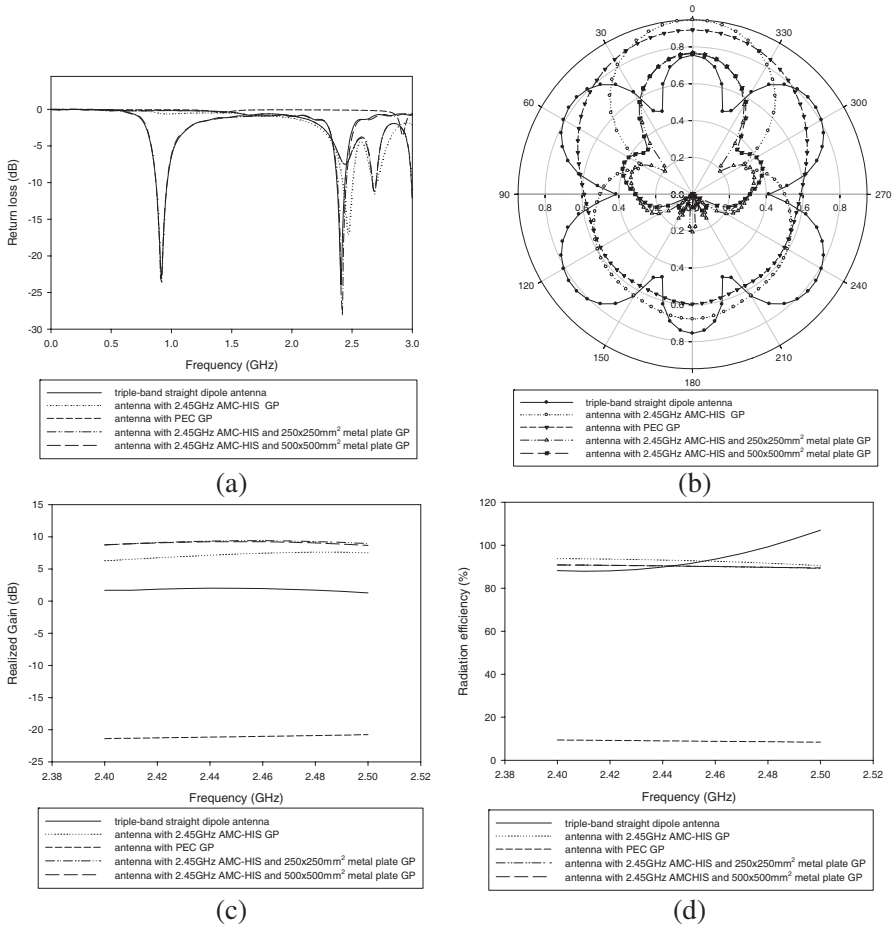

Figure 7. The performance of triple-band straight dipole antenna at 2.45 GHz: (a) return loss, (b) radiation pattern, (c) realized gain and (d) radiation efficiency.

Referring to Figure 9 and Table 5, at the preferred first working frequency, the antenna has return loss of 8.80 dB. When the antenna is incorporated with 2×1 0.92 GHz AMC-HIS, its return loss become 11.79 dB and the most important here, the realized gain and the directivity of the antenna are increased significantly from 1.49 dB and 1.93 dBi to 5.31 dB and 5.81 dBi. As data recorded in Table 5, when the antenna is attached to the PEC structure which is has same dimension of the respective AMC structure, the return loss, realized gain and radiation efficiency of the antenna are very poor. The PEC structure

at the back of the antenna acts as a reflector so that it produces high directivity to the antenna. When the designed AMC is used as a ground plane to the antenna, and then attached to the metal plate of 250 mm × 250 mm, the radiation properties such as realized gain and radiation efficiency of the antenna are remain high. The properties of the antenna are remained well when the antenna with AMC-HIS GP is attached to the bigger metal plate.

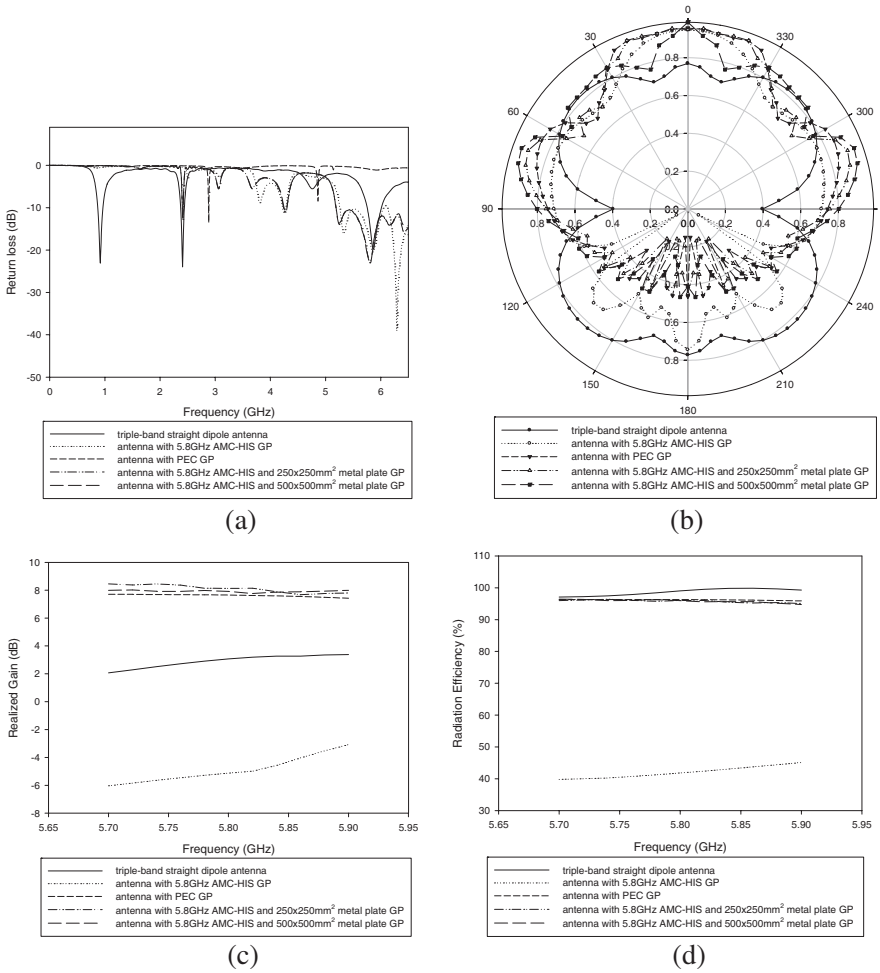

Figure 8. The performance of triple-band straight dipole antenna at 5.8 GHz: (a) return loss, (b) radiation pattern, (c) realized gain and (d) radiation efficiency.

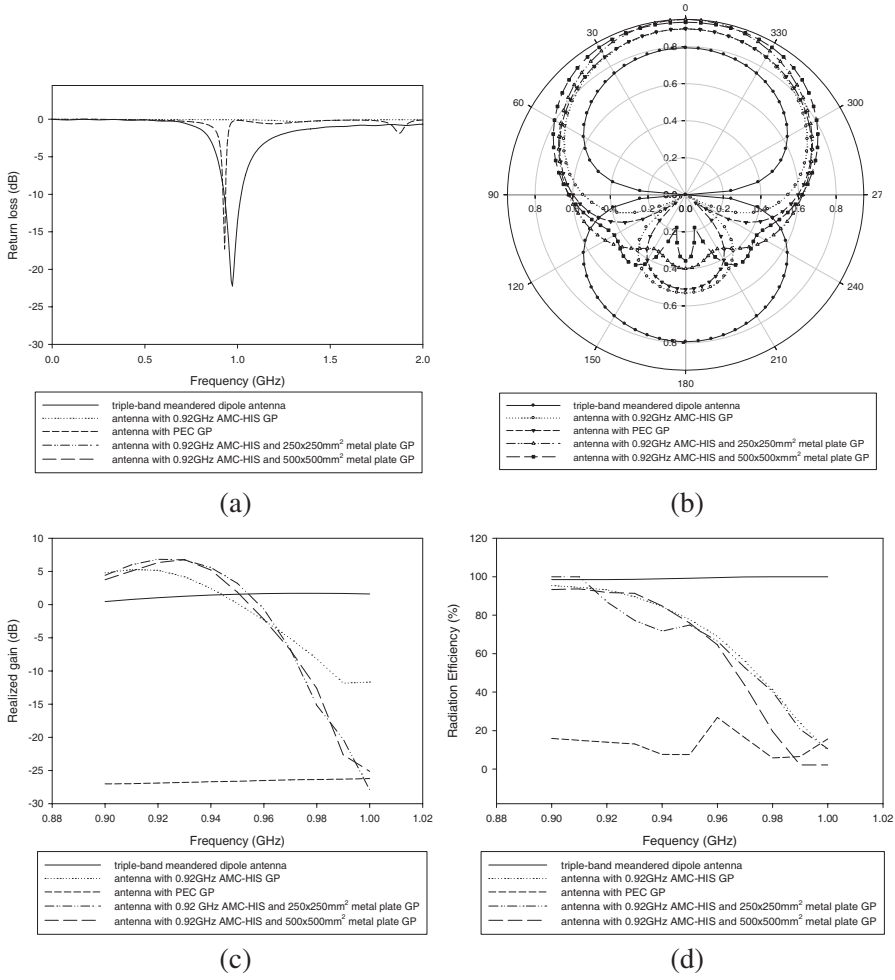

Figure 9. The performance of triple-band meandered dipole antenna at 0.92 GHz: (a) return loss, (b) radiation pattern, (c) realized gain and (d) radiation efficiency.

From Figure 9(b), it clearly shows that the radiation pattern of the dipole antenna are become directional when the antenna is attached to the respective AMC and the directivity went higher when the antenna with AMC-HIS GP is attached to the metal plate. The property of the AMC which is the reflected wave is in phase with the incident wave enhances the radiation efficiency and gives in high gain to the antenna. From the data obtained, it shows that the radiation efficiency is high, so

it produces high realized gain. The gain is increased up to 256% when the antenna is placed just above the 2×1 0.92 GHz AMC structure. This scenario or trend is showing almost similar at the middle and upper frequencies.

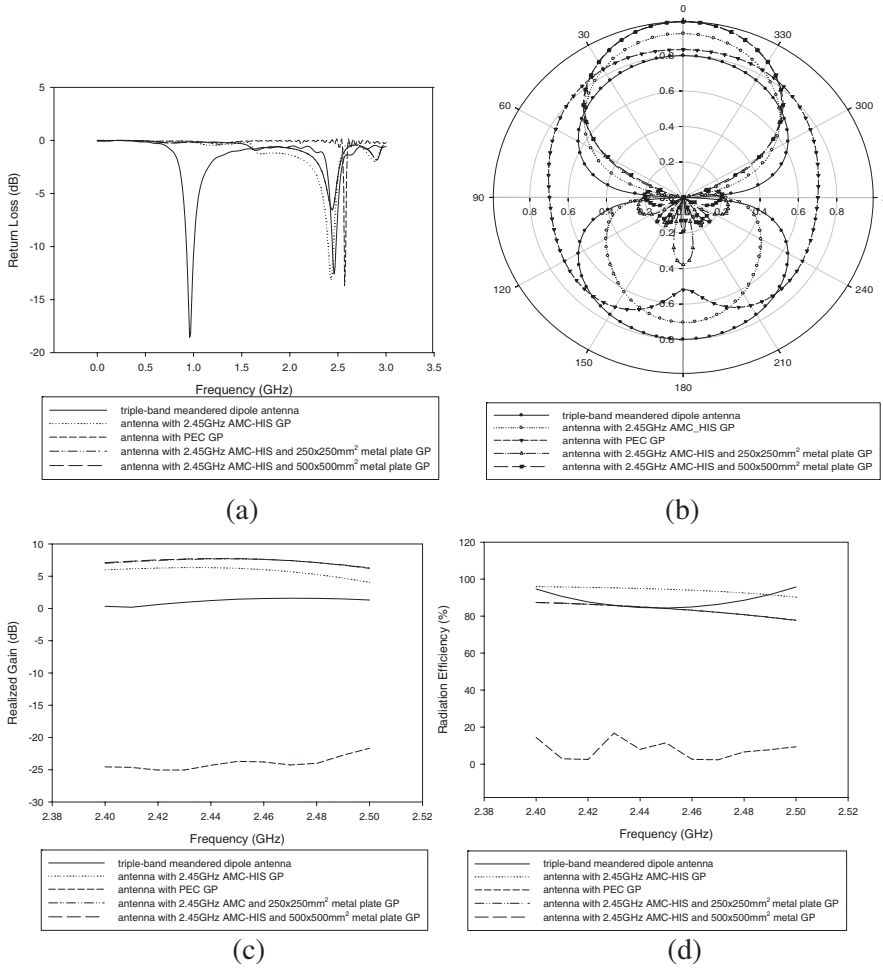

Figure 10. The performance of triple-band meandered dipole antenna at 2.45 GHz: (a) return loss, (b) radiation pattern, (c) realized gain and (d) radiation efficiency.

Table 7. The performance of triple-band meandered dipole antenna at 5.8 GHz.

	Return loss (dB)	Realized gain (dB)	Radiation Efficiency (%)	Directivity (dBi)
Triple-band meandered dipole antenna	−13.70	3.82	99.18	3.87
Triple-band meandered dipole antenna with PEC GP	−0.50	−5.62	42.68	7.75
Triple-band meandered dipole antenna with 5.8 GHz AMC-HIS GP	−13.91	7.24	96.75	7.39
Triple-band meandered dipole antenna with 5.8 GHz AMC-HIS GP and 250 mm × 250 mm metal plate	−9.43	9.93	95.99	10.11
Triple-band meandered dipole antenna with 5.8 GHz AMC-HIS GP and 500 mm × 500 mm metal plate	−9.63	8.28	96.05	8.96

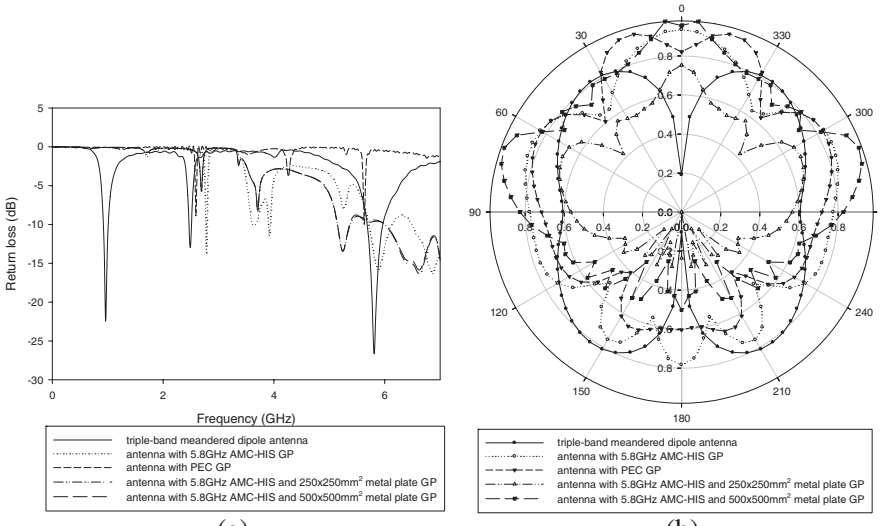

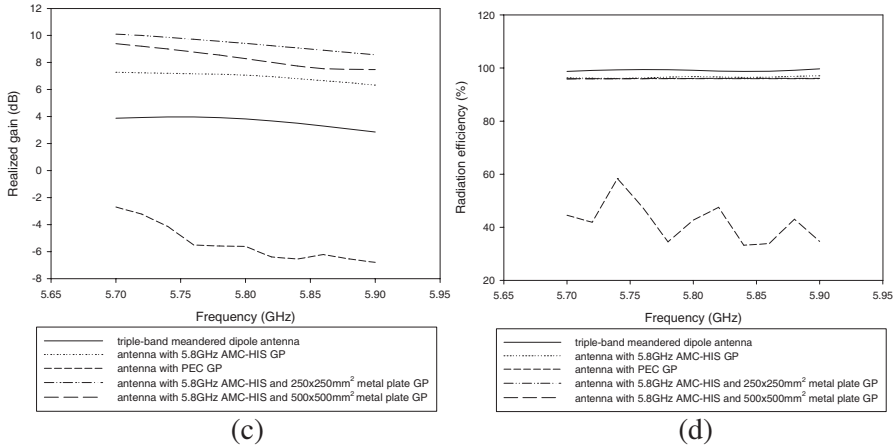

Figure 11. The performance of triple-band meandered dipole antenna at 5.8 GHz: (a) return loss, (b) radiation pattern, (c) realized gain and (d) radiation efficiency.

6. CONCLUSION

The performances of triple-band straight and meandered printed dipole antenna with and without single-band 0.92 GHz, 2.45 GHz and 5.8 GHz AMC-HIS ground plane have been analyzed in this paper. By using the AMC structure as a ground plane to the antenna, the radiation properties of the antennas are improved. The reported results show that, the realized gain, radiation efficiency and directivity are increased significantly. In this paper also, the performance of the antenna with AMC-HIS ground plane attached to the metal plate has been studied and their performances are remaining unchanged when the metal plate size is increased. In conclusion, it shows that the designed triple-band dipole tag antennas with single-band AMC-HIS can be used for metal object identifications and it can be applied at UHF and microwave frequency RFID frequency range.

7. FUTURE WORK

For future work, the proposed triple-band printed dipole antennas will be integrated with the triple-band AMC-HIS (0.92 GHz, 2.45 GHz and 5.8 GHz). Measurement of the fabricated triple-band printed dipole antenna with triple-band AMC-HIS must be carried out in order to verify the designs.

REFERENCES

1. Sievenpiper, D., L. Zhang, R. F. J. Broas, N. G. Alexopolous, and E. Yablonovitch, "High-impedance electromagnetic surfaces with a forbidden frequency band," *IEEE Trans. Microwave Theory Tech.*, Vol. 47, 2059–2074, 1999.
2. Sievenpiper, D. F., "High-impedance electromagnetic surfaces," Ph.D. Thesis, University of California at Los Angeles, 1999.
3. Poilasne, G., "Antennas on high impedance ground planes: On the importance of the antenna isolation," *Progress In Electromagnetics Research*, PIER 41, 237–255, 2003.
4. Rea, S. P., D. Linton, E. Orr, and J. McConnell, "Broadband high impedance surface design for aircraft HIRF protection," *IEE Proceeding, Microwave Antennas Propagation*, Vol. 153, No. 4, August 2006.
5. Kern, D. J., D. H. Werner, A. Monorchio, L. Lanuzza, and M. J. Wilhelm, "The design synthesis of multiband aritifial magnetic conductors using high impedance frequency selective surfaces," *IEEE Transactions on Antennas and Propagation*, Vol. 53, No. 1, 8–17, 2005.
6. Islam, S., J. Stiens, G. Poesen, I. Jaeger, G. Koers, and R. Vounckx, "W-band millimeter wave artificial magnetic conductor realization by grounded frequency selective surface," *Proceedings Symposium IEEE/LEOS Benelux Chapter*, 183–186, Brussels, 2007.
7. Zhou, X., F. Hirtenfelder, Z. Yu, and M. Zhang, "Fast simulation of high impedance surface using time domain solver," *2004 4th International Conference on Microwave and Millimeter Wave Technology Proceedings*, 731–734, 2004.
8. Yang, F. and R. Samii, *Electromagnetic Band Gap Structures in Antenna Engineering*, 156–201, Cambridge University Press, 2009.
9. Sohn, J. R., K. Y. Kim, and H.-S. Tae, "Comparative study on various artificial magnetic conductors for low-profile antenna," *Progress In Electromagnetics Research*, PIER 61, 27–37, 2006.
10. Ourir, A. and A. de Lustrac, "Artificial magnetic conductor high impedance surface for compact directive antennas," *Progress In Electromagnetics Research Symposium 2005*, 23–26, 2005.
11. Xie, H.-H., Y.-C. Jiao, K. Song, and Zhang, "A novel multi-band electromagnetic bandgap structure," *Progress In Electromagnetics Research Letters*, Vol. 9, 67–74, 2009.
12. Ayop, O., M. K. A. Rahim, M. Abu, and T. Masri, "Slotted patch dual band electromagnetic band gap structure design,"

3rd European Conference on Antennas and Propagation (EuCAP 2009), Berlin, Germany, March 23–27, 2009.

13. Abu, M., M. K. A. Rahim, M. K. Suaidi, I. M. Ibrahim, and N. M. Nor, "Dual-band artificial magnetic conductor (AMC)," *Proceedings of 2009 IEEE International Conference on Antennas, Propagation and Systems (INAS 2009)*, Johor, Malaysia, December 3–5, 2009.
14. Gu, Y.-Y., W.-X. Zhang, Z.-C. Ge, and Z.-G. Liu, "Research on reflection phase characterizations of artificial magnetic conductors," *2005 Antennas and Propagation and Microwave Conference*, APMC, 2005.
15. Lehpamer, H., *RFID Design Principles*, Artech House, 2008.
16. Chen, Z. N., *Antenna for Portable Devices*, 71–72, John Wiley & Sons, 2007.
17. Li, X., L. Yang, S.-X. Gong, Y.-J Yang, and J.-F. Liu, "A compact folded printed dipole antenna for UHF reader," *Progress In Electromagnetics Research Letters*, Vol. 6, 47–54, 2009.
18. Loo, C.-H., K. Elmahgoub, F. Yang, A. Elsherbeni, D. Kajfez, A. Kishk, and T. Elsherbeni, "Chip impedance matching for UHF RFID tag antenna design," *Progress In Electromagnetics Research*, PIER 81, 359–370, 2008.
19. Chang, K., H. Kim, K. S. Hwang, I. J. Yoon, and Y. J. Yoon, "A triple-band printed dipole antenna using parasitic elements," *Microwave and Optical Technology Letters*, Vol. 47, 221–223, 2005.
20. Wu, Y.-J., B.-H. Sun, J.-F. Li, and Q.-Z. Liu, "Triple-band omni-directional antenna for WLAN application," *Progress In Electromagnetics Research*, PIER 76, 477–484, 2007.
21. Ukkonen, L., L. Sydanheimo, and M. Kivikoski, "Patch antenna with EBG ground plane and two-layer substrate for passive RFID of metallic objects," *Proc 2004 IEEE AP-S*, Vol. 1, 93–96, 2004.
22. Ukkonen, L., L. Sydänheimo, and M. Kivikoski, "Effects of metallic plate size on the performance of microstrip patch-type tag antennas for passive RFID," *IEEE Antennas and Wireless Propagation Letters*, Vol. 4, 2005.
23. Mateos, R. M., J. M. Gonzalez, C. Craeye, and J. Romeu, "Backscattering measurement from a RFID tag based on artificial magnetic conductors," *2nd European Conference on Antennas and Propagation (EuCAP 2007)*, Edinburgh, UK, November 11–16, 2007.
24. Kim, D. and J. Yeo, "Low-profile RFID tag antenna using compact AMC substrate for metallic objects," *IEEE Antennas*

and Wireless Propagation Letters, Vol. 7, 718–720, 2008.

25. Abu, M. and M. K. A. Rahim, "Triple-band printed dipole tag antenna for RFID," *Progress In Electromagnetics Research C*, Vol. 9, 145–153, 2009.
26. John, M. and M. J. Ammann, "Integrated antenna for multiband multi-national wireless combined with GSM1800/PCS1900/IMT2000+extension," *Microwave and Optical Technology Letters*, Vol. 48, No. 3, 613–615, March 2006.